Chemical composition, pharmacodynamic activity of processed Aconitum Brachypodum Diels. and molecular docking analysis of its active target

Yanfei Niu
Southwest Forestry University
Xiaohui Li
Yunnan Institute of Materia Medica
Chunhua Wu
Southwest Forestry University
Zhengjun Shi
Southwest Forestry University
Xu Lin
Key Laboratory of State Forestry and Grassland Administration on Highly-Efficient Utilization of Forestry Biomass Resources in Southwest China
Mohamed H. Helal
Northern Border University
Ola A. Abu Ali
Taif University
Hassan Algadi
Taiyuan University of Science and Technology
Ben Bin Xu
Northumbria University
Zhe Wang (zhewang@oakland.edu)
Oakland University

Research Article

Keywords: Aconitum Brachypodum Diels., acute toxicity, pharmacodynamic activity, molecular docking

Posted Date: December 29th, 2022

DOI: https://doi.org/10.21203/rs.3.rs-2395499/v1

Additional Declarations: No competing interests reported.

Version of Record: A version of this preprint was published at Advanced Composites and Hybrid Materials on March 25th, 2023. See the published version at https://doi.org/10.1007/s42114-023-00640-5.

Abstract

Aconitum Brachypodum Diels (AB) is a plant of *Aconitum L*. The dried roots of AB have analgesic and anti-inflammatory activity. However, the processing is required to reduce toxicity before use because of its high toxicity. Studies on the toxicity, pharmacodynamics, and chemical composition of processed *Aconitum Brachypodum* Diels. (PAB) are still lacking at present. In this study, the composition changes of AB and PAB were determined by UPLC-QE-Orbitrap-MS. The intensity of diester alkaloids was greatly reduced, while the monoester alkaloids were significantly increased. An acute toxicity experiment was used to evaluate the toxicity differences between AB and PAB, while the acetic acid-induced writhing pain experiment and croton oil-induced ear edema experiment were applied to evaluate the analgesic and anti-inflammatory properties. The acute toxicity test of AB showed that the median lethal dose (LD50) was 1.37 g / kg, while the maximum tolerance of PAB was 30.0 g/kg. It was apparent that the toxicity of PAB was significantly reduced. The alkaloid component of PAB could significantly inhibit the mice's ear edema and significantly reduce the number of mice writhing. Based on the above findings, 10 compounds, including songoramine (1), neoline (2), bullatine C (3), dihydroatisine (4), bullatine A (5), maltol (6), 15-*O*-acetylsongorine (7), 15-*O*-acetylsongoramine (8), songorine (9), and aldohypaconitine (10) were separated and identified from the alkaloid component of PAB. Compounds 4, 6, 8, and 10 were firstly separate from *Aconitum*. Finally, molecular docking to anti-inflammatory analgesic target protein was carried out. The results showed that the 10 compounds and target proteins had good binding capabilities, wherein 15-*O*-acetylsongoramine could interact with the key protein Akt1 of Pi3k-Akt pathway and adjust the downstream NF-κB critical pathway to play an anti-inflammatory analgesic effect.

1. Introduction

Aconitum is a genus of Ranunculaceae [1, 2]. As a class of medicinal plants, it has a long record in Chinese history [3]. *Aconitum* plants have been shown in the literature to treat rheumatism, promote blood circulation, and disperse stasis [4]. There are about 100 species of *aconitum* in China, and they are primarily found in the southwest [5]. *Aconitum Brachypodum* Diels (AB) is a plant in the genus *Aconitum*, known as "snow grass" in China, which is bitter, acrid, warm in nature, and highly toxic. It has been recognized as having a good curative effect for relieving arthritis, dispersing blood stasis, healing wounds, promoting blood circulation, and relieving pain [6]. AB mainly contains non-alkaloid, and alkaloid components [7, 8], *β*-sitosterol, carotene, and stearic acid are the mainly non-alkaloids, and the alkaloids mainly include aconitine, hypoconitine, and artemisinin, etc. These alkaloids are mostly diterpenoids, which are currently considered to be the main components and toxic components of AB [9–11].

Aconitine is the representative highly toxic substance in *AB*, which is known to have strong cardiotoxicity and neurotoxicity [12–15]. According to literature research, aconitine can be hydrolyzed into aconine with very little toxicity during decoction. Generally, aconitine in AB is almost completely destroyed after decocting for 3 to 4 hours. Therefore, when using AB as medicine, it must be processed first. At present, the majority of research has focused on the separation and identification of active components of AB. So far, the research about processed *Aconitum Brachypodum* Diels. (PAB) are lacking.

With the development of the traditional Chinese medicine industry and material technology [16–22], traditional Chinese medicine has been developed and utilized in different application fields. For example, combining traditional Chinese medicine and material science has expanded the application direction of traditional Chinese medicine. In recent years, using cheap agricultural and forestry waste and other biomass as raw materials, and using simple and clean processes to prepare carbon materials such as activated carbon with good performance, has become a research hotspot. Some scholars have processed Chinese herbal medicine into nanoscale biological functional materials to enhance and improve the therapeutic effect of traditional Chinese medicine in various diseases [23, 24]. Some scholars have studied the applications of Chinese medicine residue in the field of composite materials, which do not pollute the environment and become a high value-added product [25, 26]. The main active component of AB is diterpene alkaloids, which have analgesic, anti-inflammatory, local anesthetic, anti-tumor and other pharmacological effects. The study of chemical components of AB and PAB can provide basic research data for the new application of this Chinese herbal medicine.

This study first reported the composition and acute toxicity of PAB. Then, alkaloid, non-alkaloid, alcohol extraction, and water extraction samples were prepared by different separation and extraction methods, and their pharmacological activities were determined. The structures of the compounds, which were isolated from the alkaloids component of PAB, were further identified. Finally, the molecular docking technology was applied, and the analgesic, anti-inflammatory protein targets were selected as a receptor to carry out molecular docking with isolated compounds, and the contribution of isolated compounds to inflammation and analgesia pharmacological activity were analyzed. Based on the research results of this paper are expected to guide the scientific processing of AB and provide data support for clinically safe drug use.

2. Materials And Methods

2.1 material

The roots of *Aconitum Brachypodum* Diels. (AB) were gathered in Huize county of Yunnan Province, P. R. China, 2018. The plant was identified by SU Tai’s group at Yunnan Institute of Materia Medica (YIMM), and the voucher specimen (20181030001) was preserved at the Department of Analysis and Testing Laboratory, YIMM, in China.

2.2 Experimental cells and animals

Mouse Mononuclear Macrophages Cells (RAW264.7) were provided by Kunming Cell Bank (cell number: KCB200603YJ). The ethical code for animal experimentation is 2021-0002. Kunming mice (weight: 18–22 g) were purchased from Beijing Hfk Bioscience Co., Ltd.

2.3 Reagents

Methanol, acetonitrile, acetic acid, ethanol, ethyl acetate, diethylamine, and CMC-Na (National Pharmaceutical Group Chemical Reagent Co., Ltd.); hydrochloric acid (Chongqing Chuandong Chemical

(Group) Co., Ltd.); $NaHCO_3$ (Xilong Chemical Co., Ltd.); $CHCl_3$, petroleum ether (Li'an Longbo Medicine Chemistry Co., Ltd.) were used. DMEM high sugar medium, fetal bovine serum, a pancreatic enzyme, and PBS buffer Gibco were provided by Thermo Fisher Scientific. TNF-α and IL-6 kits were provided by Beijing Dakewei Biotechnology Co., Ltd. Croton oil was purchased from Sigma. Acetone was obtained from Shanghai Shenbo Chemical Co., Ltd. Indomethacin was obtained from Shanghai Aladin Biochemical Technology Co., Ltd.; diclofenac diethylamine emulgel (Voltaren) was obtained from GSK Consumer Healthcare Schweiz AG.

2.4 Processing of Aconitum Brachypodum

Firstly, the roots of AB were washed, soaked in water for 20 h, then taken out, slit, and steamed at 90–100°C for 2 to 3 h. After that, AB was taken out to dry at 130°C for four h, the processed *Aconitum Brachypodum* Diels. (PAB) were thus prepared.

2.5 UPLC-QE-Orbitrap-MS Qualitative Analysis of AB and PAB

2.5.1 Sample preparation and extraction

100 μL of cold water was added to the AB and PAB samples (100 mg), and after vortexed for the 60s, 400 μL of methanol acetonitrile solution (1:1) was added and vortexed for 60s. The solutions were sonicated (30 min, 4°C, 250 W, 50 kHz) and centrifuged (12000 rpm, 20 min, 4°C).

2.5.2 UPLC Conditions

The instrument: Thermo Scientific Vanquish, UPLC, USA. The analytical conditions: HSS T3 column of Waters (1.8 μm, 100×2.1 mm), 40°C, 0.3 mL/min, 2 μL; solvent system, A was 0.1% formic acid in the water, B was acetonitrile/isopropyl alcohol (1:1, 0.1% formic acid was added); gradient program, 0.0–2.0 min (90 : 10, A : B), 6.0–15.0 min (40 : 60, A : B), 15.1–17.0 min (90 : 10, A : B).

2.5.3 QE Conditions

The instrument: QExactive, Thermo Fisher Scientific, USA; the detector: ESI. Other conditions were carried out as set by the instrument.

2.5.4 Data analysis

The raw MS data were processed by Progenesis QI. OPLS-DA was performed with SIMCA-P 14.1 software.

2.6 Acute toxicity experiment of AB and PAB

The acute toxicity experiment was used to assess the acute toxicity of AB and PAB. LD_{50} was calculated according to the previously described methods [27]. According to the result of preparation, the initial dose of AB was 2.0 g/kg, then diluted eight dose groups down based on 0.9-fold, that was 1.80, 1.62, 1.46, 1.31, 1.18, 1.06, 0.96, 0.86 g/kg, and the solvent control group which gave equal volume pure water was

established. Different doses of samples were provided by single gavage administration in 24 h, and the potential toxicity reaction and death of animals were observed.

The PAB sample was given to the mice in the highest dose (10.0 g/kg) 3 times in 24 h. There were no toxic reactions and deaths in the animals. Therefore, in the formal experiment, the maximum dose of PAB was given 3 times in 24 h (the time interval between 3 times gavage administrations was 4 h), and the possible toxicity reaction and death of animals were observed.

2.7 Pharmacological investigation

2.7.1 Extraction of different active components

2.7.1.1 Alkaloid component

After being reflux extracted 3 times by 70% ethanol from crushed PAB, it was filtered and concentrated by vacuum drying. After adding hydrochloric acid to reduce the pH of the solution to 3, ethyl acetate (EtOAc) was used to extract the concentration three times. The acidified solution was treated with ammonia water to bring them to pH 10. EtOAc was used to extract the solutions, then the extraction was concentrated under reduced pressure and dried.

2.7.1.2 Non-alkaloid component

After being reflux extracted 3 times by 70% ethanol from crushed PAB, it was filtered and concentrated by vacuum drying. After adding hydrochloric acid to reduce the pH of the solution to 3, EtOAc was used to extract the concentration three times. The extraction was concentrated under reduced pressure and dried.

2.7.1.3 Water extract component

The crushed PAB was cooked twice with water for one hour each time to extract the water-extracted components. After that, it was filtered, concentrated under reduced pressure, and dried.

2.7.1.4 Alcohol extract component

The crushed PAB was cold soaked three times with 60% ethanol solution for 24h. The collected extraction was then concentrated under reduced pressure and dried.

2.7.2 In vitro anti-inflammatory experiment

2.7.2.1 Cell culture

RAW264.7 cells were subcultured, digested with 0.25% trypsin, subcultured with DMEM high glucose medium containing 10% fetal bovine serum, and cultured at 37℃ in an incubator with 5% CO_2 saturated humidity. The solution was changed once a day, and each experiment was taken from the same passage cells.

2.7.2.2 Effects of samples on IL-6, TNF-α in Raw264.7 cells

The extracts and indomethacin were prepared into corresponding working solutions with the culture medium containing 100 μg/L LPS. RAW264.7 cells (1.0×10^5 cells/mL, 100μL/well) were inoculated for 24 h (37°C, 5% CO_2). The blank control group was added to the fresh culture medium, the LPS model group was added to a culture solution containing 100 μg/L LPS, the positive control group and the test sample group were added with the corresponding concentrations of prepared solutions, and continued to cultivate for 24 h. The ELISA kit was used to determine the levels of IL-6 and TNF-α in the supernatant.

2.7.3 In vivo anti-inflammatory experiment

Croton oil-induced ear edema was used to evaluate the anti-inflammatory activity[28]. 120 mice were randomly assigned, which included a blank control group, a positive control group (Voltaren 40 mg), and two dose groups (1 mg and 4 mg) of alkaloid, non-alkaloid, water extract, and alcohol extract. Each trial group was smeared the right ear at the volume of 0.04 mL for 3 consecutive days.

1 h after the last operation, cotton dipped in pure water was used to gently wipe the residual subject on both sides of the right ear, then 2% croton oil (20 μL) was applied to the right ear of mice to make inflammation model. After 4 h of modeling, the mice were sacrificed, and the ears were prepared into the ear tabs, the quantity of the ear tabs was weighed, and the edema degree was calculated according to Formula (1):

Ear edema = right ear quality - left ear quality (1)

2.7.4 Mice pain resistant (writhing times) experiment

Mice were divided randomly, which included a blank control group, a positive control group (Voltaren 100 mg), and two dose groups (2.5 mg and 10 mg) of alkaloid, non-alkaloid, water extract, and alcohol extract. Each day for three days, 0.1 mL of the respective group's solution was applied to the abdomen of the mice, while the solvent group received 0.1 mL of pure water.

After the last operation of 1 h, 0.62% of the acetic acid solution was injected (10 mL/kg). The writhing time intervals between 5 to 20 min after injection were recorded.

2.8 Isolation and identification of compounds from PAB

60 kg of PAB were ground into powders and extracted with 70% EtOH (three times, reflux for 2 h). Under reduced pressure, the extracting solution was concentrated at 68 L. Then, about 6 L of 7% hydrochloric acid solution was added under constant stirring to adjust the pH to about 3. After extracting with EtOAc (3×90 L), the acidified solution was treated with ammonia water to bring them to pH 10. EtOAc (380 L) was used to extract the solutions, and the resulting extract was concentrated to create the crude alkaloid fraction (475 g). Based on TLC analysis, 14 main fractions (Fr. 1–14) were obtained from the crude alkaloid fraction over silica gel (200–300 mesh) using a $CHCl_3$/MeOH (1:0–3:1, v/v) mixture with increasing polarity.

After separation and purification, The Fr.8 (10.6 g) afforded compound 1–6. The weights were 112, 320, 76, 14, 5, and 30 mg. With the aid of a similar separation process and method to the above, Fr.10 (17.1 g) afforded compounds 7 (152 mg) and 8 (60 mg), and the Fr.12 (2.7 g) provided compound 9 (12 mg) and 10 (8 mg).

Compounds were separated by classical methods, such as column chromatography and preparative liquid phase (Agilent 1100). Compounds were identified by classical methods, such as Bruker DRX-500 spectrometers (^{1}H and ^{13}C NMR spectra).

2.9 Molecular docking analysis of active target

2.9.1 Active target acquisition

Chemdraw2019 software to obtain the 3D structure of the compound, Target Prediction database such as http://www.swisstargetprediction.ch/ was used to inquire probably protein targets of analgesia and anti-inflammatory.

The String database (https://cn.string-db.org/) was used to evaluate the interactions between compound targets and anti-inflammatory analgesic interactions. The protein interaction relationship was discovered by limiting the research species to “HOMO SAPIENS” and setting the connection fraction to 0.400. Then, the interactions between targets and proteins were displayed using the Cytoscape 3.7.0 software to create PPI networks. The network topology characteristics were examined using tools for network analysis to identify important targets. As receptors, the first six targets were chosen [29].

2.9.2 Molecular docking score

The program Autodock-vina (1.1.2) was used for docking simulation, and the structures of the compounds were processed with Autodocktools (1.5.7) to minimize the energy, which was saved as a pdbqt file. The top six targets were used to conduct the semi-flexible molecule docking with the corresponding compound, and the score of each receptor and compound was obtained.

2.9.3 Molecular docking visualization

Opening Pymol 2.3.0 and discovery studio client were used to visualize the docking results. 15-*O*-Acetylsongoramine was chosen as a representative compound based on the aforementioned key target selection experiment to examine the specific binding between 15-*O*-acetylsongoramine and each target, and the visualized molecular docking figures were obtained.

2.10 Statistical analysis

The data was analyzed using SPSS 17.0 statistical software, and the experimental results were represented by $x \pm s$. The level of the inspection was $\alpha = 0.05$. The acute toxicity experimental LD_{50} and 95% were calculated using Bliss [30].

3. Results And Discussion

3.1 UPLC-QE-Orbitrap-MS Qualitative Analysis of AB and PAB

The positive total ion chromatogram of AB and PAB (Fig. 1) showed that the chemical composition changed significantly. The *t*-test was used to combine the multivariate analysis of OPLS-DA, and different metabolites were screened (VIP > 1 and $P < 0.05$). The variation trend of the intensity of the alkaloid component in AB and PAB (Fig. 2) showed that the diester alkaloids (aconitine, hypaconitine, 3-acetylaconitine, and 3-deoxyaconitine) were significantly reduced, while the monoester alkaloids (14-benzoylaconine, benzoylhypaconine, benzoylmesaconine) and aconine were significantly increased.

After retrieving the NiH Chemid Plus chemical toxic database, after mouse intravenous injection aconitine, hypaconitine, 3-acetylaconitine, LD_{50} were 0.10, 0.47, 0.4 mg/kg, 14-benzoylaconine, benzoylhypaconine, benzoylmesaconine were 10.1, 23, 21 mg/kg, and aconine was 117 mg/kg. After the mouse abdominal injection 3-deoxyaconitine, the LD_{50} was 1.9 mg/kg. The above LD50 was normalized and then multiplied by the respective response intensity to obtain the virulence values in the form of a heat map (Fig. 3). From the perspective of total toxicity, the poison value of AB was higher than the PAB significantly.

These results showed that the toxicity of AB decreased after processing. From the perspective of various components, aconitine was accounted for a significant portion of the toxicity contributions, suggesting the toxicity reduction mechanism of PAB. It was closely related to the decrease in aconitine content and was consistent with the literature reports[31–33].

3.2 Acute toxicity experiment

As shown in Table 1, all animals were generally good in the control group, and there was no obvious abnormal reaction or death. In the AB group, the maximum tolerance was 0.86 g/kg with no animal death. The mice's minimum lethal death of the AB was 0.96 g/kg, with animal mortality of 10%. Additionally, the lethality increased in a gradient with increasing AB dose. All mice died when the AB dose was 2 g/kg. The LD_{50} of AB was 1.37 g/kg, and the 95% confidence interval was 1.28 ~ 1.46 g/kg. Anatomical observation of animal death during the observation period did not reveal significant abnormalities.

In the PAB group, some mice showed a mild toxic reaction, mainly diarrhea, and no significant toxic reactions or death were observed throughout the observation period. Therefore, we concluded that the maximum tolerance of PAB was 30.0 g/kg.

Table 1
Animal toxicity reaction and death of AB and PAB.

group	dose (g/kg)	Total number of mice	number of mice death	mortality rate/%	LD_{50} and 95% confidence interval
control	-	10	0	0	-
AB	2.00	10	10	100	
	1.80	10	9	90	
	1.62	10	8	80	
	1.46	10	4	40	
	1.31	10	2	20	1.37 g/kg
	1.18	10	3	30	(1.28 ~ 1.46 g/kg)
	1.06	10	2	20	
	0.96	10	1	10	
	0.86	10	0	0	
PAB	30.0	10	0	0	-

3.3 Pharmacological investigation

3.3.1 In vitro anti-inflammatory experiment

As shown in Fig. 4 and Fig. 5, the alkaloid components of PAB at concentrations of 2.5 μg/mL, 5 μg/mL, and 10 μg/mL significantly reduced both contents of TNF-α and IL-6, compared with the model group ($P < 0.05$). In addition, the non-alkaloid component of PAB with a concentration of 10 μg/mL and the water extract component of PAB (0.5 μg/mL) significantly decreased both levels. The alcohol extract component of PAB significantly reduced the content of IL-6 at a concentration of 2 μg/mL ($P < 0.05$), however, there was no effect on the content of TNF-α significantly. These results suggest that some components of PAB might substantially alleviate the inflammatory response of cells induced by LPS.

3.3.2 In vivo anti-inflammatory experiment (croton oil-induced ear edema)

As shown in Fig. 6, the Voltaren (positive control, 40 mg) and alkaloid component of PAB (4 mg) significantly decreased the mice's ear edema ($P < 0.05$) after continuous 3 days. In contrast, the non-alkaloid component of PAB, alcoholic extract component of PAB, and alcoholic extract component of PAB did not decrease the mice's ear edema. Therefore, we speculate that PAB plays an anti-inflammatory role mainly through the alkaloid component.

3.3.3 Mice pain resistant (writhing times) experiment

To detect the analgesic effect of PAB component, we conducted the mice pain-resistant experiment. As shown in Table 2 and Fig. 7, there were no significant effects on the body weight of mice compared to the control group ($P > 0.05$). After 3 days, the Voltaren (positive control, 100 mg) and alkaloid component (10 mg) significantly reduced the number of writhing in mice ($P < 0.05$) and displayed an obvious analgesic effect. The non-alkaloid component of PAB, the water extract component of PAB and the alcohol extract component of PAB did not significantly affect the writhing of mice.

Table 2
Effects of different extracts on the number of mice writhing and weight.

group	dose (mg/animal)	body weight (g)	writhing time (s)
control	-	26.3 ± 1.4	31.83 ± 9.50
voltaren	100	25.7 ± 2.0	22.58 ± 16.70*
alkaloid	2.5	26.7 ± 2.8	23.42 ± 18.97
	10	26.5 ± 1.4	18.42 ± 11.07*
non-alkaloid	2.5	26.3 ± 2.0	26.17 ± 16.85
	10	26.0 ± 1.7	24.92 ± 18.77
water extract	2.5	25.8 ± 1.4	25.00 ± 14.73
	10	25.8 ± 1.6	26.00 ± 13.01
alcohol extract	2.5	25.4 ± 1.0	29.00 ± 10.77
	10	26.3 ± 1.6	25.67 ± 17.45

3.4 Isolation and identification of compounds from PAB

Overall, NMR and MS were used to determine the structures. Firstly, ten compounds (Fig. 8) were isolated and purified from PAB using chromatographic techniques such as HPD100 and preparative HPLC. Subsequently, physicochemical data and modern spectral analysis techniques were used to identify their structures, which were songoramine (1), neoline (2), bullatine C (3), dihydroatisine (4), bullatine A (5), maltol (6), 15-*O*-acetylsongorine (7), 15-*O*-acetylsongoramine (8), songorine (9), and aldohypaconitine (10). For the first time, compounds 4, 6, 8, and 10 were isolated from this plant.

3.4.1 Songoramine

White amorphous powder; $C_{22}H_{29}NO_3$, ESI-MS *m/z*356 $[M + H]^+$; ^1H NMR (MeOD, 500MHz, Supplementary Table S1**)**; ^{13}C NMR (MeOD, 125MHz, Supplementary Table S2). The comparative analysis [34, 35]

verified that the obtained compound **1** was songoramine.

3.4.2 Neoline

White amorphous powder; $C_{24}H_{39}NO_6$, ESI-MS *m/z*438 $[M + H]^+$; ^1H NMR (MeOD, 500MHz, Supplementary Table S1); ^{13}C NMR (MeOD, 125MHz, Supplementary Table S2). After comparative analysis [34–36], which verified that the obtained compound **2** was neoline.

3.4.3 Bullatine C

White amorphous powder; $C_{26}H_{41}NO_7$, ESI-MS *m/z*480 $[M + H]^+$; ^1H NMR (MeOD, 500MHz, Supplementary Table S1); ^{13}C NMR (MeOD, 125MHz, Supplementary Table S2). After comparative analysis [36], which verified that the obtained compound **3** was bullatine C.

3.4.4 Dihydroatisine

White amorphous powder; $C_{22}H_{35}NO_2$, ESI-MS *m/z*346 $[M + H]^+$; ^1H NMR ($CDCl_3$, 500MHz) δ_H: 0.81 (3H, s, H-18), 2.31 (2H, d, J = 11.0Hz, H-19), 2.66 (2H, m, H-21), 3.59 (1H, brs, H-15), 3.69 (2H, t, J = 5.5Hz, H-22), 5.08, 5.02 (1H each, t, J = 1.5Hz, H-17); ^{13}C NMR ($CDCl_3$, 125MHz, Supplementary Table S2). After comparative analysis [37, 38], which verified that the obtained compound **4** was dihydroatisine.

3.4.5 Bullatine A

White needle crystal; $C_{22}H_{33}NO_2$, ESI-MS *m/z*344 $[M + H]^+$; ^1H NMR (Pyridine-d_5, 500MHz Supplementary Table S1); ^{13}C NMR (Pyridine-d_5, 125MHz, Supplementary Table S2). After comparative analysis [39], which verified that the obtained compound **5** was bullatine A.

3.4.6 Maltol

Colorless needle crystal; $C_6H_6O_3$, ESI-MS *m/z*127 $[M + H]^+$; ^1H NMR ($CDCl_3$, 500MHz) δ_H: 2.35 (3H, s, 2-CH_3), 6.41 (1H, d, J = 5.5Hz, H-6), 7.69 (1H, d, J = 5.5Hz, H-5); ^{13}C NMR ($CDCl_3$, 125MHz) δ_C: 173.1 (C-4), 154.2 (C-6), 149.2 (C-2), 143.3 (C-3), 113.2 (C-5), 14.3 (2-CH_3). After comparative analysis [40], which verified that the obtained compound **6** was maltol.

3.4.7 15-O-acetylsongorine

Colorless square crystal; $C_{24}H_{33}NO_4$, ESI-MS *m/z*400 $[M + H]^+$; ^1H NMR (MeOD, 500MHz, Supplementary Table S1); ^{13}C NMR (MeOD, 125MHz, Supplementary Table S2). After comparative analysis [41], which verified that the obtained compound **7** was 15-*O*-acetylsongorine.

3.4.8 15-O-acetylsongoramine

Powder (white, amorphous); $C_{24}H_{31}NO_4$, ESI-MS *m/z*398 $[M + H]^+$; ^1H NMR (MeOD, 500MHz) δ_H: 2.08 (1H, dd, J = 16.0, 6.5Hz, H-11), 2.10 (3H, s, 15-$OCOCH_3$), 2.66, 2.76 (1H each, dq, J = 12.0, 7.0Hz, H-21), 2.98 (1H, d, J = 1.5Hz, H-20), 3.73 (1H, s, H-19), 4.03 (1H, d, J = 5.5Hz, H-1), 4.93 (1H, t, J = 2.0Hz, H-17), 5.64

(1H, t, *J* = 2.5Hz, H-15); ^{13}C NMR (MeOD, 125MHz, Supplementary Table S2). After comparative analysis [42], which demonstrated that the obtained compound **8** was 15-*O*-acetylsongoramine.

3.4.9 Songorine

Powder (white, amorphous); $C_{22}H_{31}NO_3$, ESI-MS *m/z*358 $[M + H]^+$; ^{1}H NMR (MeOD, 500MHz, Supplementary Table S1); ^{13}C NMR (MeOD, 125MHz, Supplementary Table S2). After comparative analysis [34, 35], which demonstrated that the obtained compound **9** was songorine.

3.4.10 Aldohypaconitine

Powder (white, amorphous); $C_{33}H_{43}NO_{11}$, ESI-MS *m/z*630 $[M + H]^+$, 652 $[M + Na]^+$; ^{1}H NMR ($CDCl_3$, 500MHz) δ_H: 1.34 (3H, s, 8-$OCOCH_3$), 2.68 (1H, brs, H-7), 3.21 (3H, s, 1-OCH_3), 3.29 (3H, s, 6-OCH_3), 3.94 (1H, brs, H-17), 3.96 (1H, s, 13-OH), 4.08 (1H, d, *J* = 7.0Hz, H-6), 4.27 (1H, d, *J* = 3.0Hz, 15-OH), 4.49 (1H, dd, *J* = 5.0, 3.0Hz, H-15), 4.89 (1H, d, *J* = 5.0Hz, H-14), 7.46 (2H, brt, *J* = 7.5Hz, H-3', 5'), 8.02 (2H, brd, *J* = 7.5Hz, H-2', 6'), 8.09 (1H, s, N-CHO); ^{13}C NMR ($CDCl_3$, 125MHz, Supplementary Table S2). After comparative analysis [43, 44], which demonstrated that the isolated compound **10** was aldohypaconitine.

3.5 Molecular docking analysis of active target

Six core target proteins in the network—AKT1, JUN, PTGS2, PIK3CA, SLC6A2, and SLC6A3 were conducted via virtual molecular docking verification based on the findings of Autodock Vina's protein interaction network analysis. The combinations of semi-flexible molecules that correspond to the six target proteins selected as receptors were determined (Table 3). A strong binding capability is indicated by a score of less than − 5 kcal/mol; the lower the score value, the more potent the binding ability [44, 45]. The molecular docking score revealed that ten active compounds exhibited strong binding properties with their respective target proteins, indicating that 10 compounds are more responsible for PAB's analgesic and anti-inflammatory actions. Combined with the result of key target protein semi-flexible molecular docking, 15-*O*-acetylsongoramine and AKT1, JUN, PTGS2, PIK3CA and SLC6A3 target proteins had better affinity, and their binding ability scores were − 9.5, -7.8, -7.6, − 7.8 and − 7.6 kcal/mol, respectively, which were less than − 7 kcal/mol, indicating that 15-*O*-acetylsongoramine had a strong binding ability with key targets. The binding ability of 15-*O*-acetylsongoramine and target SLC6A2 were − 5.3 kcal/mol, which showed that 15-*O*-acetylsongoramine can interact with the target SLC6A2. The molecular docking visualization of 15-*O*-acetylsongoramine and six main target proteins was also carried out (Fig. 9). AKT1, JUN, PTGS2, PIK3CA, SLC6A2, and SLC6A3 all have molecular surfaces that can embed 15-*O*-acetylsongoramine, which binds to the active pocket of the protein to form a stable complex. And then, according to the interaction 2D graph analysis, the hydroxyl group of 15-*O*-acetylsongoramine formed a hydrocarbon bond with THR473 of AKT1 protein; the methyl group and the methylene group of 15-*O*-acetylsongoramine formed Pi-Alkyl/Alkyl interaction with PRO387, HIS547, TRP84, LEU89 and PHE472 in AKT1 protein. And 15-*O*-acetylsongoramine formed van der Waals interaction with ARG85 ASP313 LYS92 and ASP476 in AKT1 protein. These interactions promote 15-*O*-Acetylsongoramine to be well bonded to the active cavity of the AKT1 protein. The Akt1 protein, a crucial component of the Pi3k-Akt

pathway, interacted with 15-*O*-acetylsongoramine to inhibit the regulation of its activity, affecting the critical NF-κB pathway downstream and having an anti-inflammatory effect.

Table 3
AutoDock vina calculation results of ligand and receptor (kcal/mol).

compounds	AKT1	JUN	PTGS2	PIK3CA	SLC6A2	SLC6A3
Songoramine	-9.5	-7.4	-6.8	-7.5	-6.9	-8.1
Neoline	-7.2	-6.8	-6.7	-5.9	-5.2	-6.7
Bullatine C	-7.3	-6.7	-6.8	-6.1	-3.6	-7.1
Dihydroatisine	-8.9	-7.2	-6.4	-6.3	-6.5	-7.2
Bullatine A	-8.7	-7.3	-6.6	-6.7	-4.7	-7.4
Maltol	-5.2	-4.3	-5.5	-4.7	-5.3	-5.1
15-*O*-acetylsongorine	-9.3	-7.4	-6.8	-6.5	-4.7	-7.9
15-*O*-acetylsongoramine	-9.5	-7.8	-7.6	-7.8	-5.3	-7.6
Songorine	-9	-7.8	-7.1	-6.3	-4.7	-7.4
Aldohypaconitine	-8.6	-7.1	-7.4	-7.5	-2.0	-7.8

4. Conclusions

In this study, AB was processed to PAB, and the alkaloid component, non-alkaloid component, water extract component, and alcohol extract component of AB and PAB were prepared. After that, the chemical composition, acute toxicity, and pharmacological activity were measured. There were mainly eight different alkaloid components in both AB and PAB, with PAB including lower diester alkaloids and higher monoester alkaloids, which suggests that the toxicity components of PAB were reduced. And the acute toxicity experiment also showed that LD_{50} to mice of AB was 1.37 g/kg, but PAB only showed low toxicity to mice. Analgesia, anti-inflammatory experimental results showed that the alkaloid component, non-alkaloid component, water extract component, and alcohol extract component of PAB have *in vitro* anti-inflammatory effects. The alkaloid component of PAB showed certain *in vivo* anti-inflammatory and analgesic effects. Finally, ten compounds were separated from the alkaloid component of PAB, and then docked to analgesic, active anti-inflammatory targets through molecular docking techniques. The results showed that the separated ten compounds have significant contributions to analgesia and anti-inflammatory activity. Especially 15-*O*-acetylsongoramine, could affect the effect of anti-inflammatory analgesia by participating in the adjustment of Pi3k-Akt and NF-κB pathway.

Declarations

Fundings

The authors gratefully acknowledge financial support from the Major science and technology project-Biomedicine Major special project of Yunnan province, China (2018ZF011), the National Natural Science Foundation of China (32160414), the Key Laboratory of State Forestry and Grassland Administration on Highly-Efficient Utilization of Forestry Biomass Resources in Southwest China (2020-KF14). The authors extend their appreciation to the Deputyship for Research& Innovation, Ministry of Education in Saudi Arabia, for funding this research work through project number “IF_2020_NBU_239”.

Author Contributions Statement

C.W. and Z.W. have designed this project and contributed to the main manuscript text. Y.N. conducted experiments and wrote the main manuscript text. X.L., Z.S., X.L., O.A.A.A., H.A., M.H., and B.B.X. have contributed to conducting the experiments, preparing figures, and writing. All authors reviewed the manuscript.

Conflict of interest

The authors declare no competing interests.

References

1. Li Y, Meng Y, Shen SK, Wang Y (2012) Karyological Studies of Aconitum brachypodum and Related Species. Cytologia 77(4):491–498. https://doi.org/10.1508/CYTOLOGIA.77.491
2. Shen Y, Zuo AX, Jiang ZY, Zhang XM, Wang HL, Chen JJ (2015) Two New Diterpenoid Alkaloids from Aconitum brachypodum. Die Pharmazie 13(12):390–393. https://doi.org/10.5012/bkcs.2010.31.11.3301
3. Singhuber J, Zhu M, Prinz S, Kopp B (2009) Aconitum in traditional Chinese medicine: a valuable drug or an unpredictable risk? Journal of Ethnopharmacology 126(1):18–30. https://doi.org/10.1016/j.jep.2009.07.031
4. Luo HF, Wang H, Huang XD, Wang YZ (2008) Preparation and in vitro Evaluation of Compound Aconitum brachypodum Patches. Chinese Journal of Pharmaceuticals(09):662–666. https://doi.org/10.3969/j.issn.1001-8255.2008.09.010
5. Hao DC, Gu XJ, Xiao PG, Xu L, Peng Y (2013) Recent advances in the chemical and biological studies of Aconitum pharmaceutical resources. J Chin Pharm Sci 22(3):209–221. https://doi.org/10.5246/jcps.2013.02.030
6. Yang L, Zhang Y, Mei S, Zhu Z (2019) Diterpenoid alkaloids from the roots of Aconitum brachypodum Diels. And their chemotaxonomic significance. Biochemical Systematics and Ecology 85:43–45. https://doi.org/10.1080/10286020.2016.1173677
7. Xiao PG, Wang FP, Gao F, Yan LP, Chen DL, Liu Y (2006) A pharmacophylogenetic study of Aconitum L.(Ranunculaceae) from China. Journal of Systematics and Evolution 44(1):1. https://doi.org/10.1360/aps050046

8. Wang X, Wang D, Lai G, Zhou Z, Wang Y (2018) Diterpenoid Alkaloids from Aconitum brachypodum. Chemistry of Natural Compounds 54(1):137–141. https://doi.org/10.1080/10286020.2016.1173677
9. Yang LG, Zhang YJ, Xie JY, Xia WJ, Zhang HY, Tang MY, Mei SX, Cui T, Wang JK, Zhu ZY (2016) Diterpenoid alkaloids from the roots of Aconitum brachypodum Diels. Journal of Asian natural products research 18(9):908–912. https://doi.org/10.1080/10286020.2016.1173677
10. Shen Y, Zuo AX, Jiang ZY, Zhang XM, Wang HL, Chen JJ (2010) Four new nor-diterpenoid alkaloids from Aconitum brachypodum. Helvetica Chimica Acta 93(5):863–869. https://doi.org/10.1002/hlca.200900297
11. Huang YF, He F, Cui H, Zhang YY, Yang HY, Liang ZS, Dai W, Cheng CS, Xie Y, Liu L (2022) Systematic investigation on the distribution of four hidden toxic Aconitum alkaloids in commonly used Aconitum herbs and their acute toxicity. Journal of Pharmaceutical and Biomedical Analysis 208:114471. https://doi.org/10.1016/j.jpba.2021.114471
12. Ge YB, Jiang Y, Zhou H, Zheng M, Li J, Huang XJ, Gao Y (2016) Antitoxic effect of Veratrilla baillonii on the acute toxicity in mice induced by Aconitum brachypodum, one of the genus Aconitum. Journal of ethnopharmacology 179:27–37. https://doi.org/10.1016/j.jep.2015.12.030
13. Fraser SP, Salvador V, Manning EA, Mizal J, Altun S, Raza M, Berridge RJ, Djamgoz MBA (2003) Contribution of functional voltage-gated Na + channel expression to cell behaviors involved in the metastatic cascade in rat prostate cancer: I. Lateral motility. Journal of cellular physiology 195(3):479–487. https://doi.org/10.1002/jcp.10312
14. Belgium LB, Handley UA, Marsden UA, Germany RA, Ameri A (1998) The effects of Aconitum alkaloids on the central nervous system. Progress in Neurobiology 56(2):211–235. https://doi.org/10.1016/S0301-0082(98)00037-9
15. Chan TYK (2009) Aconite poisoning. Clinical toxicology 47(4):279–285. https://doi.org/10.1080/15563650902904407
16. Hu W, Huang J, Zhang X, Zhao S, Pei L, Zhang C, Liu Y, Wang Z (2020) A mechanically robust and reversibly wettable benzoxazine/epoxy/mesoporous TiO2 coating for oil/water separation. Appl Surf Sci 507:145168. https://doi.org/10.1016/j.apsusc.2019.145168
17. Wang Z, Zhu H, Cao N, Du R, Liu Y, Zhao G (2017) Superhydrophobic surfaces with excellent abrasion resistance based on benzoxazine/mesoporous SiO2. Mater Lett 186:274–278. https://doi.org/10.1016/j.matlet.2016.10.010
18. Zhu H, Hu W, Xu Y, Wang B, Zheng D, Fu Y, Zhang C, Zhao G, Wang Z (2019) Gradient structure based dual-robust superhydrophobic surfaces with high-adhesive force. Appl Surf Sci 463:427–434. https://doi.org/10.1016/j.apsusc.2018.08.241
19. Zhu Q, Zhao Y, Miao B, Abo-Dief HM, Qu M, Pashameah RA, Xu BB, Huang M, Algadi H, Liu X, Guo Z (2022) Hydrothermally synthesized ZnO-RGO-PPy for water-borne epoxy nanocomposite coating with anticorrosive reinforcement. Prog Org Coat 172:107153. https://doi.org/10.1016/j.porgcoat.2022.107153

20. Yu Z, Yan Z, Zhang F, Wang J, Shao Q, Murugadoss V, Alhadhrami A, Mersal GAM, Ibrahim MM, El-Bahy ZM, Li Y, Huang M, Guo Z (2022) Waterborne acrylic resin co-modified by itaconic acid and γ-methacryloxypropyl triisopropoxidesilane for improved mechanical properties, thermal stability, and corrosion resistance. Prog Org Coat 168:106875. https://doi.org/10.1016/j.porgcoat.2022.106875
21. Xu J, Zhu P, El Azab IH, Bin Xu B, Guo Z, Elnaggar AY, Mersal GAM, Liu X, Zhi Y, Lin Z, Algadi H, Shan S (2022) An efficient bifunctional Ni-Nb2O5 nanocatalysts for the hydrodeoxygenation of anisole. Chinese Journal of Chemical Engineering 49:187–197. https://doi.org/10.1016/j.cjche.2022.07.009
22. Zhang Y, Cao L, Fu H, Zhang M, Meng J, Althakafy JT, Abo-Dief HM, El-Bahy SM, Zhang Y, Wei H, Xu BB, Guo Z (2022) Effect of sulfamethazine on anaerobic digestion of manure mediated by biochar. Chemosphere 306:135567. https://doi.org/10.1016/j.chemosphere.2022.135567
23. Feng YH, Li XL, Jin G, Qu JP, He HZ (2015) Preparation and properties of several Chinese herbal residue/polylactic acid composites. J Thermoplast Compos Mater 28(2):214–224. https://doi.org/10.1177/0892705713475369
24. Wang JY, Yang FX, Chen CW, Wang GL, Chai L, Chen ZG (2022) Preparation and properties of anisic acid/catechin modified polypropylene bacteriostatic film. Journal of Functional Materials 53(02):2174–2181. https://doi.org/10.3969/j.issn.1001-9731.2022.02.026
25. Wei SM, Wang YH, Tang ZS, Wang Z, Zhang Z, Su R, Jin RY, Song ZX (2020) Study on the reduction of silver nano and antioxidant and bacteriostatic activities by the residue of Yinqiao detoxification mixture. Chinese Traditional and Herbal Drugs 51(16):4169–4175. https://doi.org/10.7501/j.issn.0253-2670.2020.16.009
26. Wang YH, Zou TY, Su R, Wei SM (2022) Study on the preparation of nanosilver and anticancer effect in vitro by the green preparation of slag of slag. Chinese Traditional and Herbal Drugs 53(07):1964–1972. https://doi.org/10.7501/j.issn.0253-2670.2022.07.005
27. Li QX, Wang H, Xiao QQ, Kong R (1995) Evaluation and calculation of Median Lethal Dose (LD50)Bliss method. Journal of Mathematical Medicine(04):318–320. https://doi.org/CNKI:SUN:SLYY.0.1995-04-009
28. Kelechi M, Uzoma AI (2015) Anti-inflammatory Activities of the Leaf Chloroform Extract of Palisota hirsuta. Journal of Advances in Medical and Pharmaceutical Sciences 2:57–63. https://doi.org/10.9734/JAMPS/2015/13813
29. Li JS, Zhao ZZ, Miao XD, Su SL, Shang EX, Qian DW, Duan JA (2021) Study on the mechanism of frankincense-myrrh compatibility in improving rheumatoid arthritis based on network pharmacology-molecular docking. Chinese Journal of Chinese Materia Medica 46(10):2371–2379. https://doi.org/10.19540/j.cnki.cjcmm.20201126.401
30. Zhang C, Yi Y, Chen J, Xin R, Yang Z, Guo Z, Liang J, Shang R (2015) In vivo efficacy and toxicity studies of a novel antibacterial agent: 14-o-[(2-amino-1,3,4-thiadiazol-5-yl)thioacetyl] mutilin. Molecules 20(4):5299–5312. https://doi.org/10.3390/molecules20045299
31. Lu G, Dong Z, Wang Q, Qian G, Huang W, Jiang Z, Leung KSY, Zhao Z (2010) Toxicity assessment of nine types of decoction pieces from the daughter root of Aconitum carmichaeli (Fuzi) based on the

chemical analysis of their diester diterpenoid alkaloids. Planta medica 76(08):825–830. https://doi.org/10.1055/s-0029-1240688

32. Zhang DK, Han X, Li RL, Niu M, Zhao YL, Wang JB, Yang M, Xiao XH (2016) Analysis of the differences of chemical components in Fuzi from different habitats by UPLC-Q-TOF-MS. China Journal of Chinese Materia Medica 41(3):463–469. https://doi.org/10.4268/cjcmm20160318
33. Peter K, Schinnerl J, Felsinger S, Brecker L, Bauer R, Breiteneder H, Xu R, Ma Y (2013) A novel concept for detoxification: complexation between aconitine and liquiritin in a Chinese herbal formula ('Sini Tang'). Journal of ethnopharmacology 149(2):562–569. https://doi.org/10.1016/j.jep.2013.07.022
34. Csupor D, Forgo P, Csedő K, Hohmann J (2006) C19 and C20 Diterpene Alkaloids from Aconitum toxicum RCHB. Helvetica Chimica Acta 89(12):2981–2986. https://doi.org/10.1002/hlca.200690267
35. He CJ, Li XH, Geng Z, Yang L, Guo L, Peng C (2014) Chemical constituents of n-butanol extract from aconite. Chinese Traditional Patent Medicine 36(05):1004–1007. https://doi.org/10.3969/j.issn.1001-1528.2014.05.026
36. Zhao B, Zhao JY, Sagdullaev S, Aisa HA (2018) Diterpene alkaloids from Aconitum smirnovii. Chemistry of Natural Compounds 54(4):828–830. https://doi.org/10.1007/s10600-018-2490-0
37. Mody NV, Pelletier SW (1978) 13C nuclear magnetic resonance spectroscopy of atisine and veatchine-type C20-diterpenoid alkaloids from aconitum and garrya species. Tetrahedron 34(16):2421–2431. https://doi.org/10.1016/0040-4020(78)88367-7
38. Yang LH, Chun LI, Lin LM, Wang ZM, Zhong LI (2016) Fat-soluble Alkaloids from Aconitum tanguticum. Chinese Journal of Experimental Traditional Medical Formulae 22(10):32–36. https://doi.org/10.1007/s10600-018-2490-0
39. Wang HY, Zuo AX, Sun Y, Rao GX (2013) Chemical constituents of Aconitum brachypodum from Dong-Chuan area. China Journal of Chinese Materia Medica 38(24):4324–4328. https://doi.org/10.4268/cjcmm20132426
40. Li RR, Yuan ST, Li ZH, Qin HL (2005) Studies on chemical constituents in Flos Sophorae Carbonisatus. China journal of Chinese materia medica 30(16):1255–1257. https://doi.org/10.3321/j.issn:1001-5302.2005
41. Fan ZC, Zhang ZQ (2008) Molecular and crystal structure of 15-acetylsongorine and songoramine isolated from Aconitum szechenyianum Gay. Structural Chemistry 19(3):413–419. https://doi.org/10.1007/s11224-008-9296-9
42. Gao F, Li YY, Wang D, Huang X, Liu Q (2012) Diterpenoid alkaloids from the Chinese traditional herbal "Fuzi" and their cytotoxic activity. Molecules 17(5):5187–5194. https://doi.org/10.3390/molecules17055187
43. Wei DH, Wang F, Song B, Cui JC, Song XM, Yue ZG (2015) Diterpenoid alkaloids from Aconitum Penduli Radix and their bioactivities. Chin J Exp Tradit Med Form 21:48–52. https://doi.org/10.13422/j.cnki.syfjx.2015190048
44. Wang X, Zhao T, Lai S (1995) Alkaloids of cultivated Aconitum carmichaeli I. Chinese Pharmaceutical Journal-Beijing 30:716–718

45. Zuo WM, Li JP, Li CM, Wang HY, Liu LK, Zeng Y (2021) UPLC-Q-TOF-MS / MS Combined with Network Pharmacology and Molecular Docking to Explore the Anti-hepatitis Substances and Mechanism of Halenia Ellipta. Natural Product Research And Development 33(11):1946–1956. https://doi.org/10.16333/j.1001-6880.2021.11.018

Figures

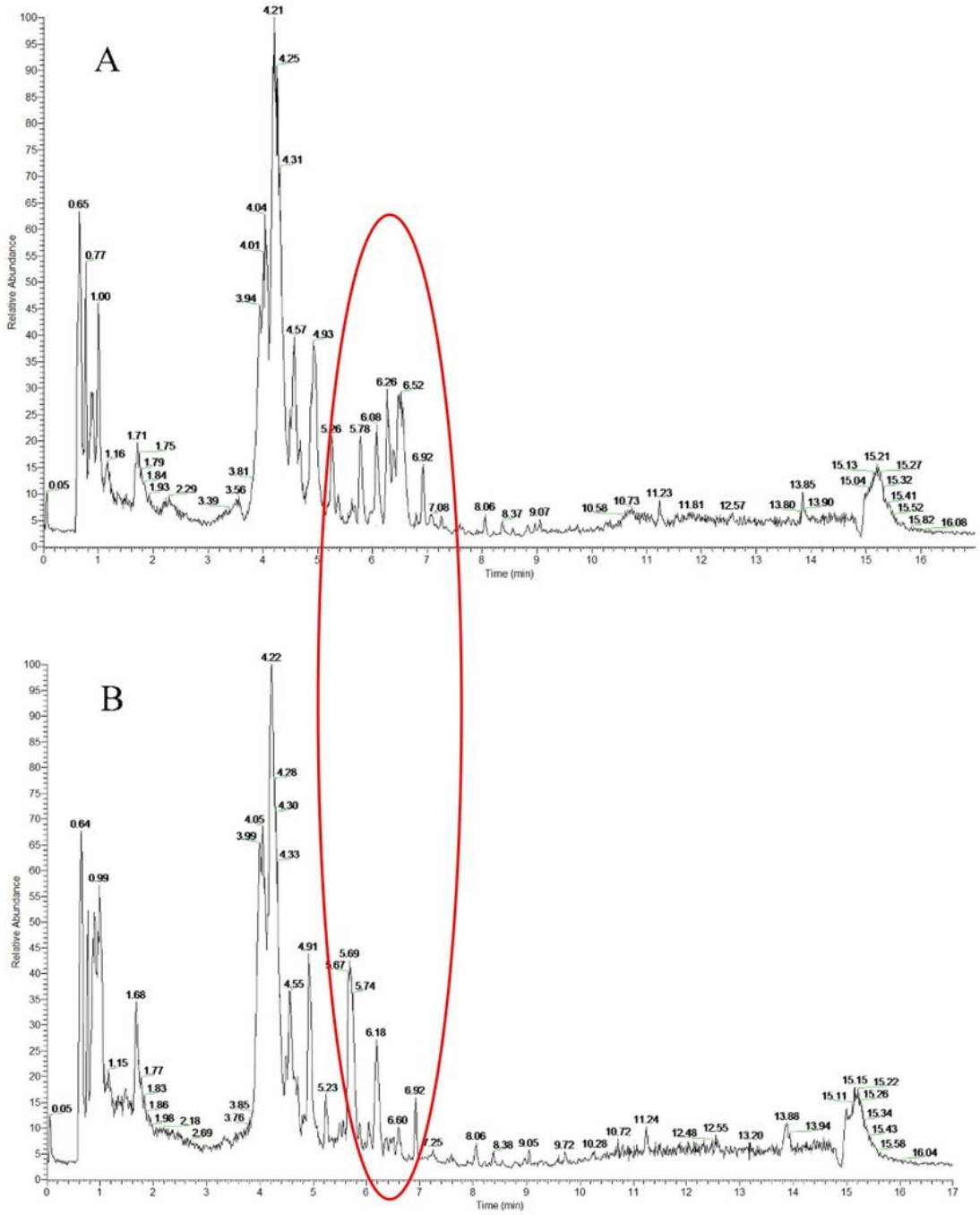

Figure 1

Positive total ion chromatograms for (A) AB solution; (B) PAB solution.

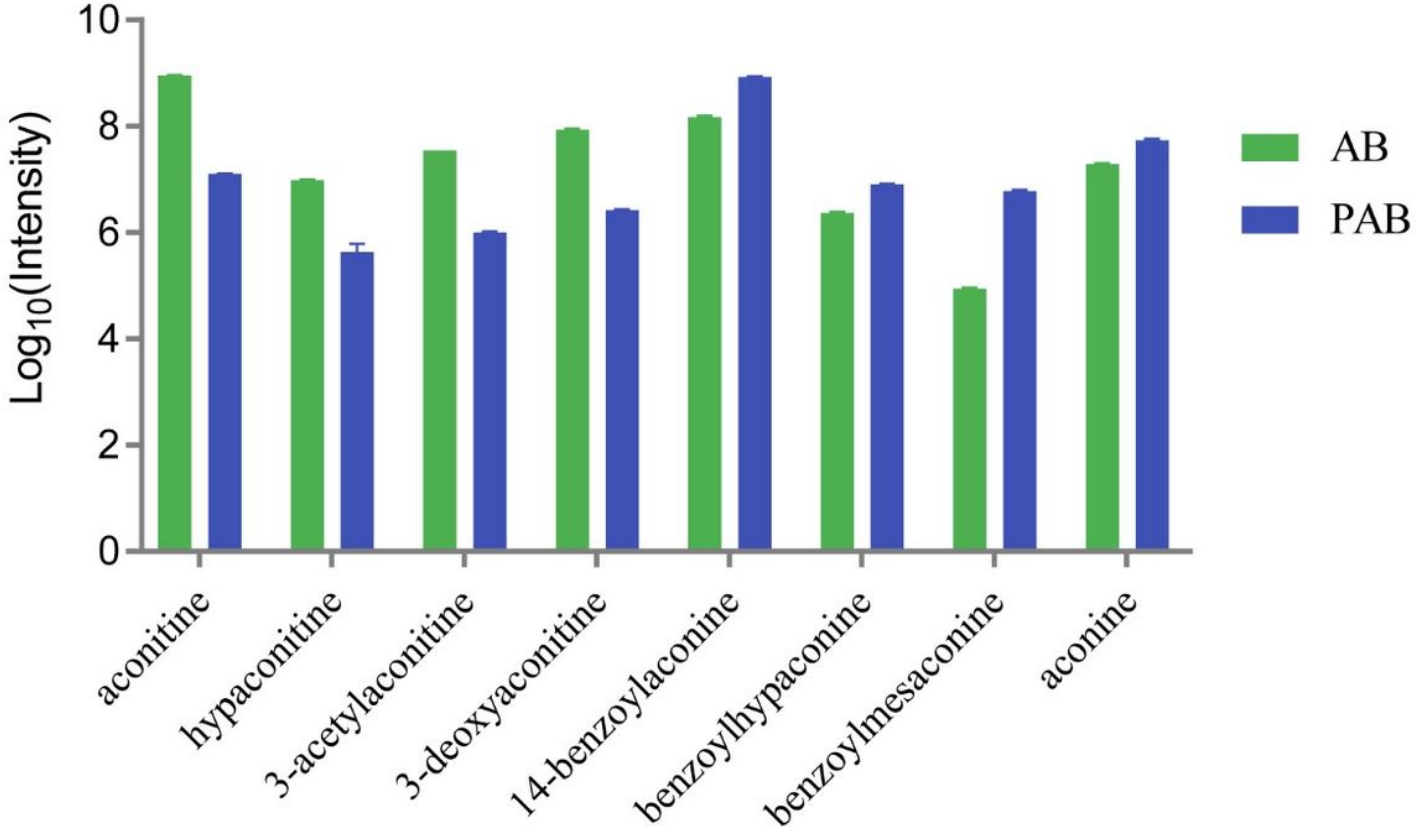

Figure 2

The variation trend of the intensity of the alkaloid component in AB and PAB.

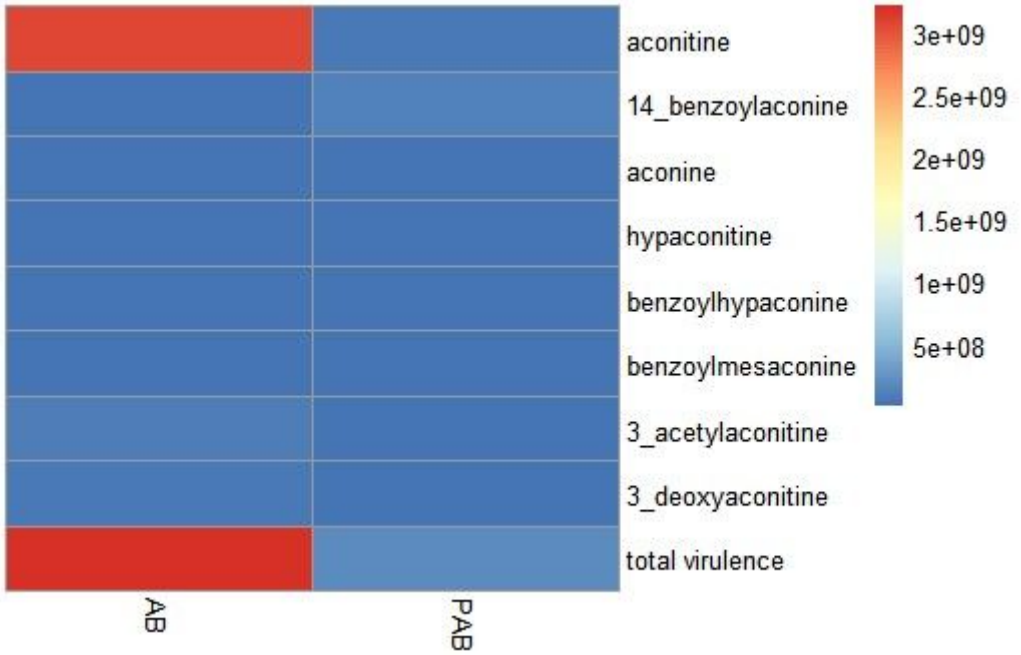

Figure 3

Virulence thermograph of main metabolic markers in AB and PAB.

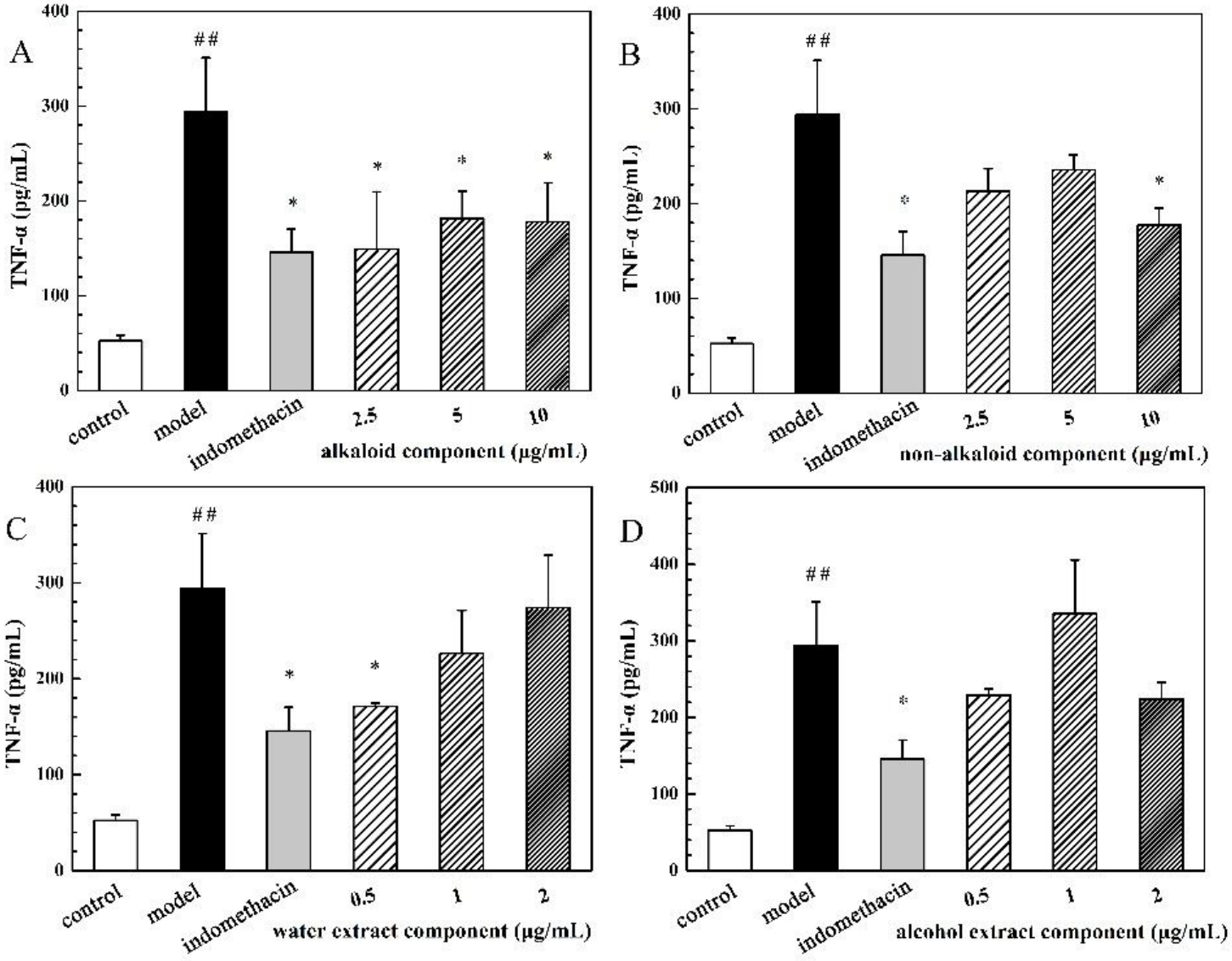

Figure 4

Effects of different extracts on TNF-α content (n= 5). (*P <0.05 versus model group, ##P< 0.01 versus blank control group) A. alkaloid component; B. non-alkaloid component; C. water extract component; and D. alcohol extract component.

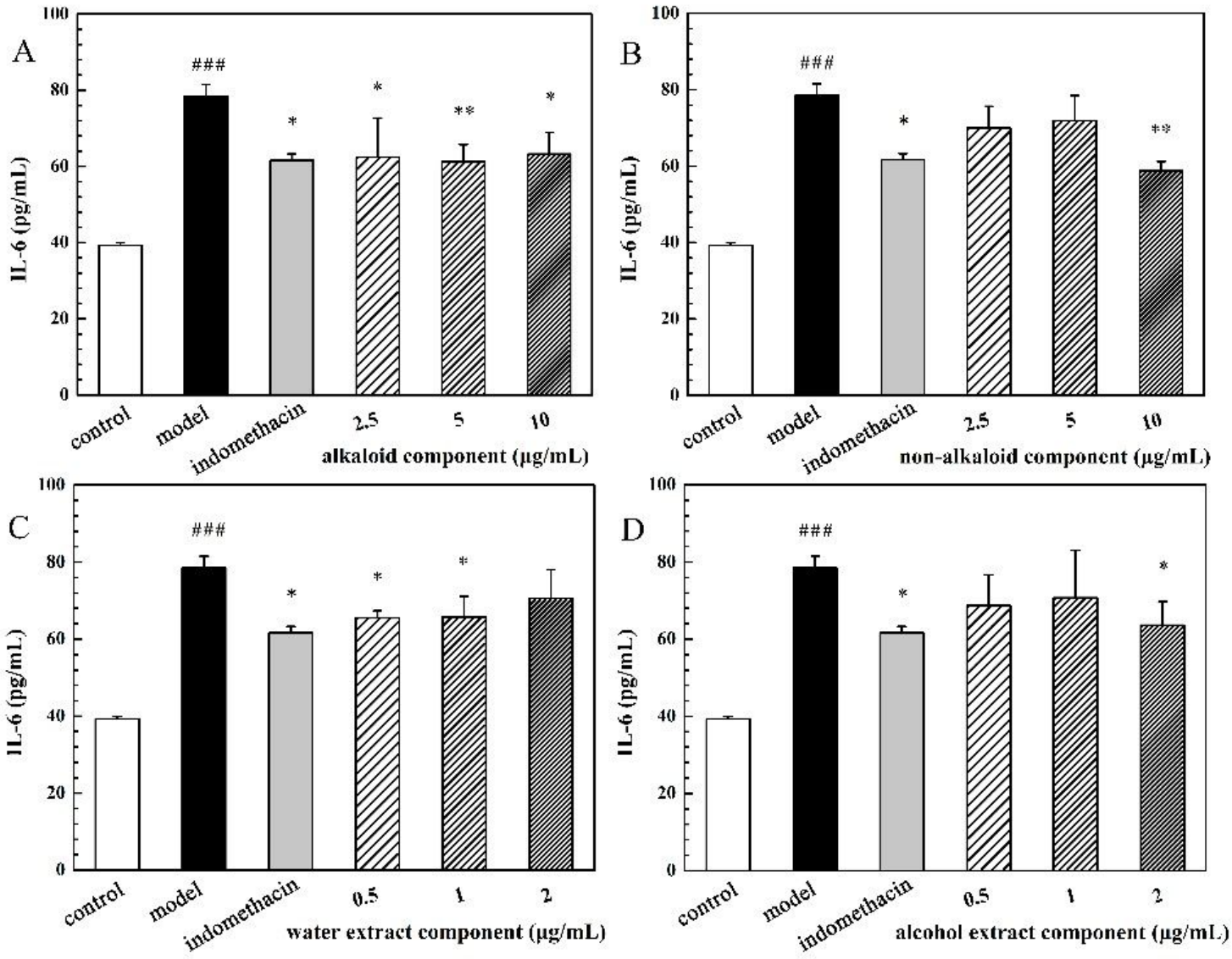

Figure 5

Effects of different extracts on IL-6-α content (n= 5). (*P <0.05 versus model group, ###P<0.001 versus blank control group). A. alkaloid component; B. non-alkaloid component; C. water extract component; and D. alcohol extract component.

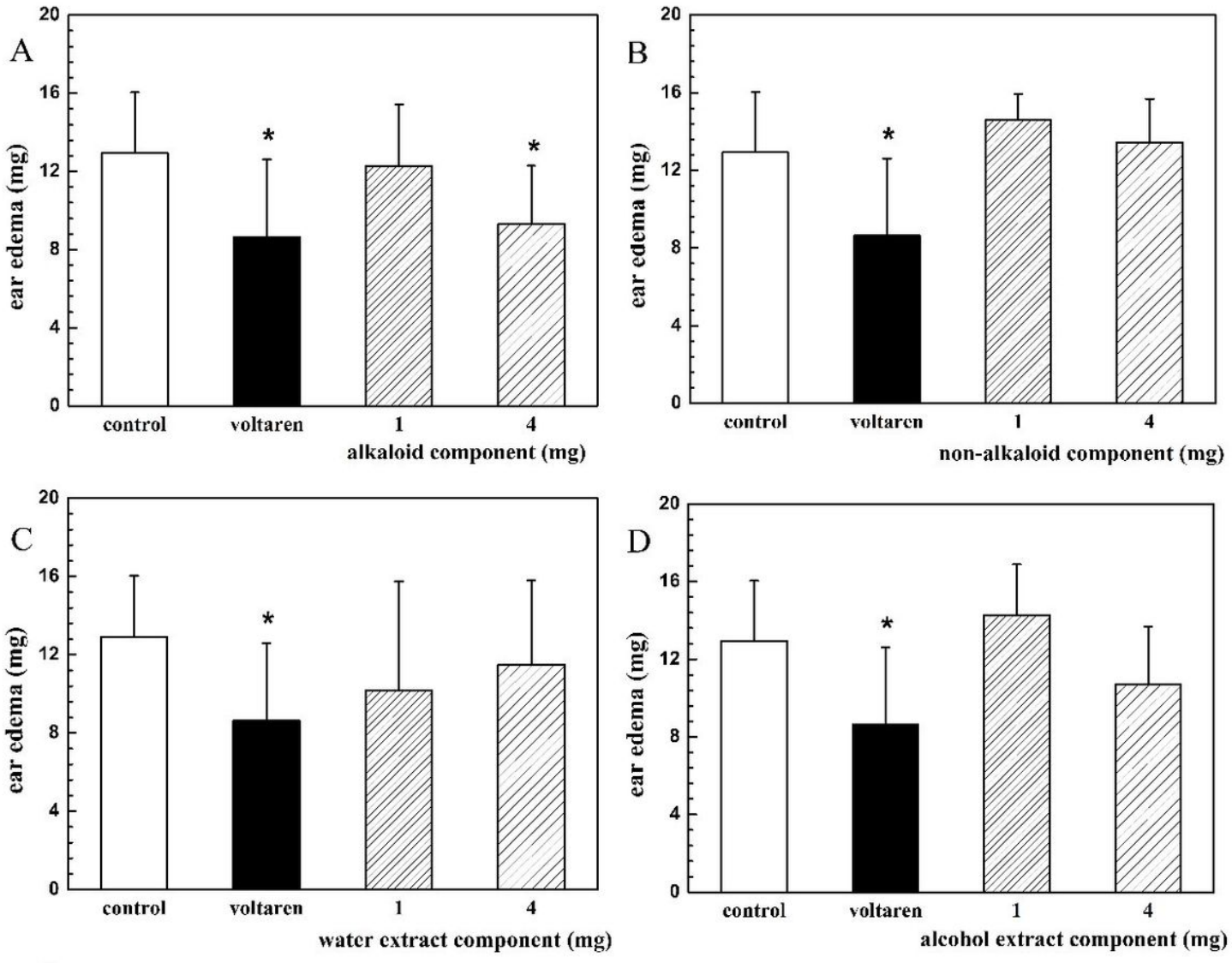

Figure 6

Effects of different extracts on mice ear edema after topical drug delivery (n= 12). (*P < 0.05 versus blank control group) A. alkaloid component; B. non-alkaloid component; C. water extract component; and D. alcohol extract component.

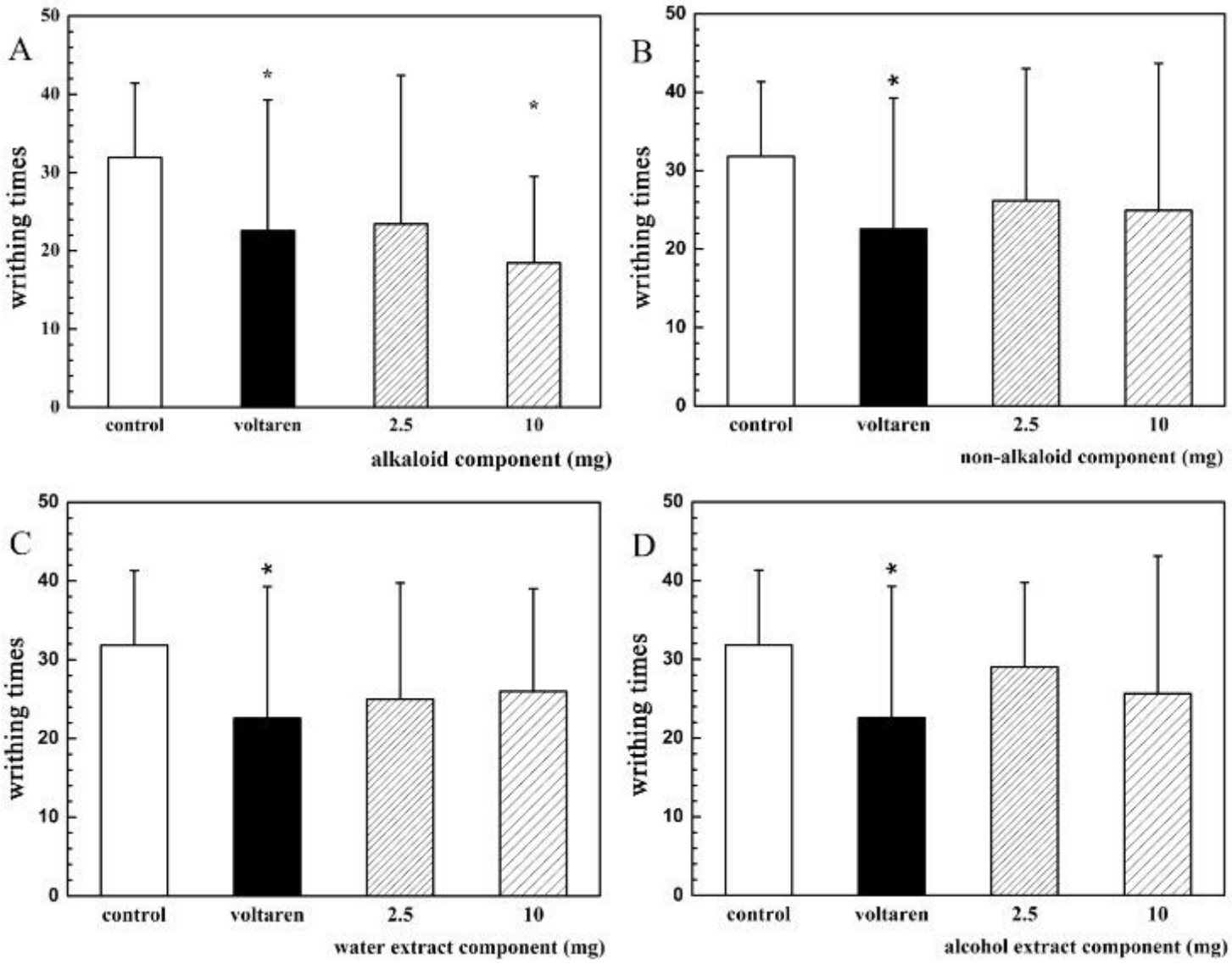

Figure 7

Effects of different extracts on the number of mice twist after topical drug delivery (n= 12). (*$P < 0.05$ versus blank control group) A. alkaloid component; B. non-alkaloid component; C. water extract component; and D. alcohol extract component.

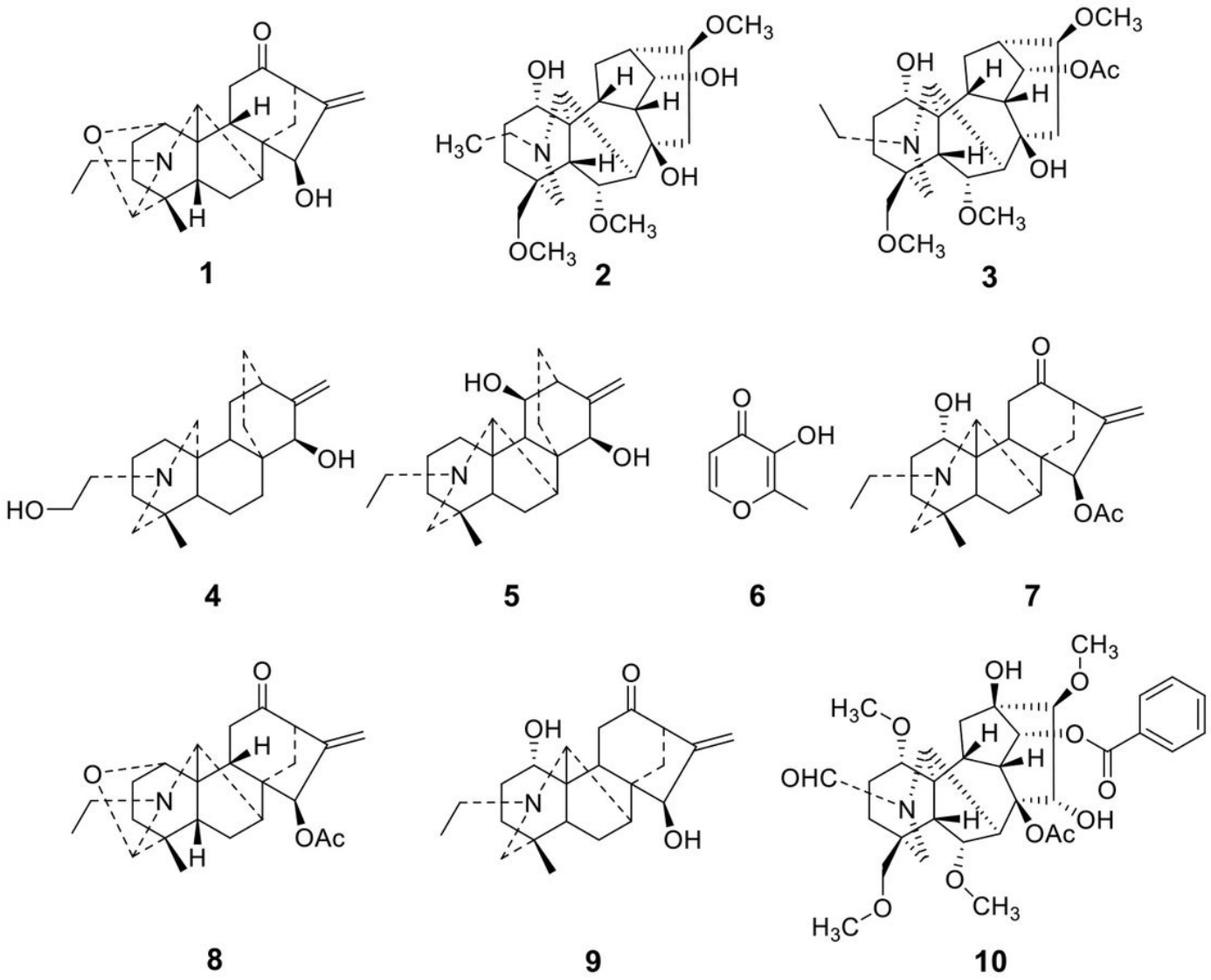

Figure 8

The structures of compounds 1-10.

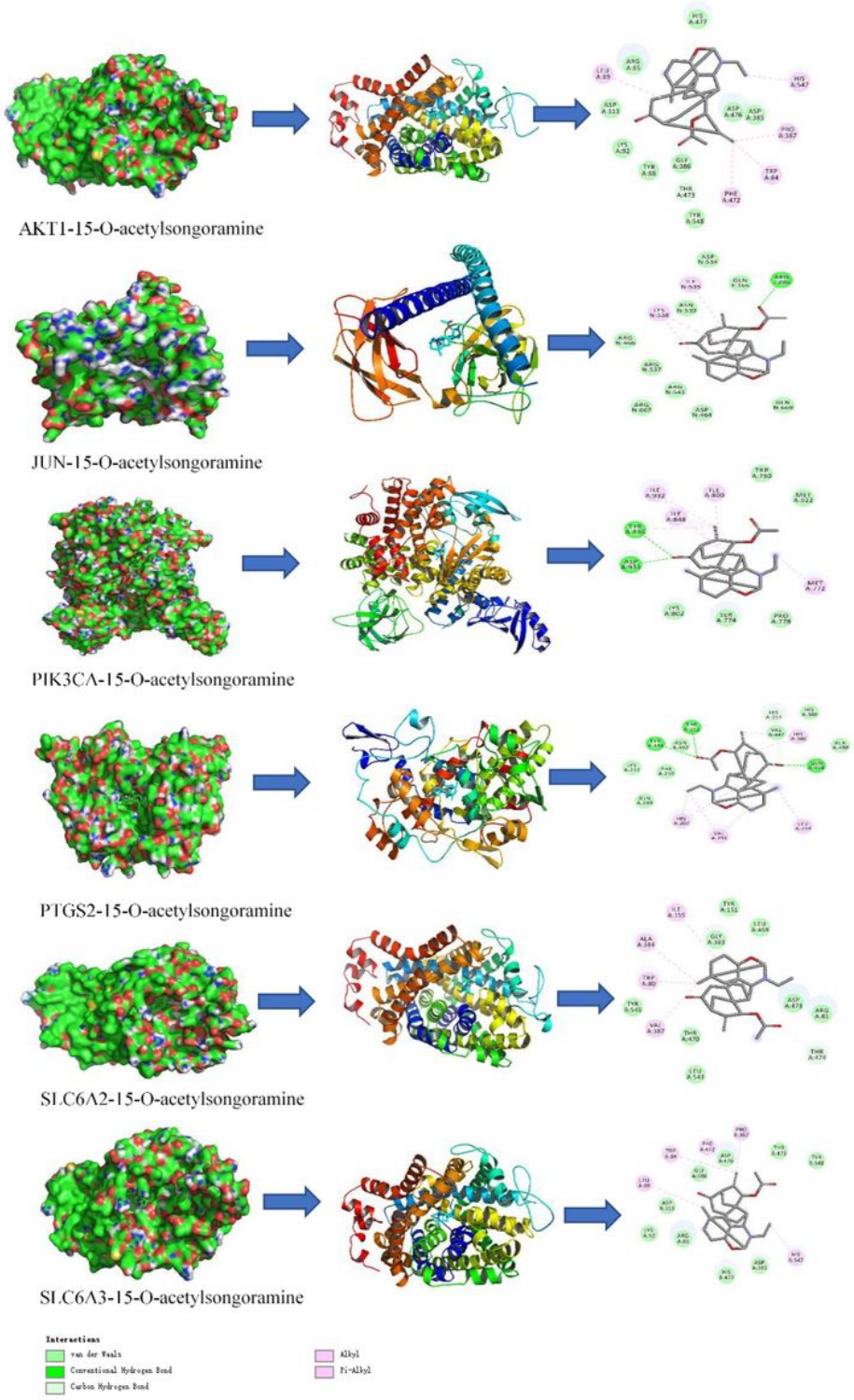

Figure 9

Molecular docking map of 15-*O*-acetylsongoramine and targets.

Supplementary Files

This is a list of supplementary files associated with this preprint. Click to download.

- Image.jpg
- supportinginformation.docx